Journal of Catalysis **196,** 126–133 (2000)
doi:10.1006/jcat.2000.3005, available online at http://www.idealibrary.com on IDEAL®

The Room Temperature, Stoichiometric Conversion of N_2O to Adsorbed NO by Fe-MCM-41 and Fe-ZSM-5

Gerd Grubert,*[,1] Michael J. Hudson,† Richard W. Joyner,*[,2] and Michael Stockenhuber*[,2]

*Catalysis Research Laboratory, Department of Chemistry and Physics, Nottingham Trent University, Clifton Lane, Nottingham NG11 8NS, United Kingdom; and †Department of Chemistry, University of Reading, Box 224, Whiteknights, Reading RG6 6AD, United Kingdom

Received April 25, 2000; revised July 10, 2000; accepted July 17, 2000

Nitrous oxide (N_2O) interacts at room temperature and low pressure ($>10^{-5}$ mbar) with Fe(II) species in both Fe-MCM-41 and Fe-ZSM-5, to form adsorbed nitric oxide. The adsorbed product is identified by its characteristic but different N=O stretching frequencies on these two materials, and also by chemiluminescent analysis after desorption at $T > 420$ K. It is proposed that the other product of N_2O decomposition is nitrogen. This decomposition is thermodynamically favourable, due not least to the heat of adsorption of the adsorbed NO formed. Catalytic N_2O decomposition, forming nitrogen and oxygen, does not occur until $T > 770$ K, probably by a different mechanism.

Key Words: **nitrous oxide (N_2O); conversion to nitric oxide (NO); MCM-41; Fe-ZSM-5; iron.**

1. INTRODUCTION

Nitrogen has a very rich oxide chemistry, forming oxides in which it exhibits all of the formal oxidation states from one to five. Although all are thermodynamically unstable with respect to decomposition into their constituent elements, they usually display high kinetic stability and are pernicious atmospheric contaminants. Most attention has focused on nitric oxide and its atmospheric oxidation products NO_2 and N_2O_4 (NOx). However, nitrous oxide (N_2O) is a greenhouse gas which is liberated into the atmosphere in a number of ways, including de-NOx treatments, combustion of fossil fuels and biomass, and adipic acid production.

There is an extensive literature on the catalytic decomposition of nitrous oxide into its elements, and this reaction can be carried out with varying degrees of efficiency by many simple oxides (1, 2) and also by transition metal exchanged zeolites (3–6). The recognition that N_2O can be a significant by-product of the selective catalytic reduction of NOx by hydrocarbons, particularly when platinum is an important catalytic component, has generated renewed interest in nitrous oxide decomposition (7).

With others (8), we are also interested in the use of nitrous oxide as an oxidant with transition-metal-containing porous catalysts such as Fe-ZSM-5 and Fe-MCM-41 (9, 10). We here report the observation, surprising but unambiguous, that these materials convert nitrous oxide into adsorbed nitric oxide at room temperature.

2. EXPERIMENTAL

Si-MCM-41 was prepared in a heterogeneous system following the procedure of Grün *et al.* (11). Cetyltriammoniumbromide (CTAB, Aldrich, 99%, 2.4 g) was dissolved in water (120 ml) at 299 K, followed by the addition of ammonia solution (8 ml, 25%) and tetraethylorthosilicate (TEOS, Aldrich, 98%, 10 ml). After the solution was stirred for 1 h, the precipitated sample was dried overnight at 353 K and calcined at 823 K for 12 h. To introduce iron and/or aluminum atoms during the synthesis, $Fe(NO_3)_3 \cdot 9H_2O$ (0.95 g) and/or $Al(NO_3)_3 \cdot 9H_2O$ (1.12 g) were added to the CTAB–water solution. To achieve a better distribution of the metal atoms in the framework of the MCM-41, TEOS was added before the ammonia, as it is known to form a complex with the metal ion. The samples prepared by this method are designated Fe-MCM-41-SYN and Al-MCM-41-SYN.

Alternatively, iron was introduced into MCM-41 after framework synthesis, using iron acetylacetonate [$Fe(acac)_3$] in toluene, a method developed by Kenvin and white for the preparation of iron oxide species on silica (12). Si-MCM-41 (5 g) was dispersed in toluene (Aldrich 99.8%, 200 ml), $Fe(acac)_3$ (Aldrich 99%, 1.5 g) was added, and the mixture was stirred at room temperature for 24 h. After filtration and washing the resulting material was calcined at 823 K for 12 h, and this material is designated Fe-MCM-41-PS.

Iron was introduced into H-ZSM-5 using a triple-exchange process described previously (13). For each exchange, H-ZSM-5 (3 g) was slurried for 24 h at room

[1] Present address: Institut für Angewandte Chemie Berlin-Adlershof e.V., Richard-Willstätter-Str. 12, 12484 Berlin, Germany.

[2] To whom correspondence should be addressed. R.W.J.: Fax: 44-115-948-6838. E-mail: richard.joyner@ntu.ac.uk. M.S.: Fax: (44)-115-948-6694. E-mail: michael.stockenhuber@ntu.ac.uk.

0021-9517/00 $35.00

temperature in an iron nitrate solution (500 ml, 0.1 M) and subsequently dried at 373 K.

The structures of the MCM-41-derived materials were characterised by X-ray diffraction using a Spectrolab CP5 Series 3000.120 powder diffractometer with nickel-filtered Cu $K\alpha$ radiation, physical adsorption of nitrogen (Micromeritics, ASAP 2000), and transmission electron microscopy (TEM) using a Philips CM20 instrument operating at 200 keV. The materials were also examined by *in situ* infrared spectroscopy. An ATI Research Series FTIR spectrometer measuring in transmission mode was equipped with a reaction chamber which has also been described before (13). Samples were initially activated at 773 K in a vacuum (10^{-7} mbar), in air, or in hydrogen. To allow quantitative comparisons, absorptions were normalised using overtone lattice vibrations with frequencies between 2200 cm^{-1} and 1700 cm^{-1} (14). The intensities of the overtone bands in these MCM-41 samples correspond well with the literature (15), and are also used to obtain an estimation of the relative wafer thickness of ZSM-5 samples. The validity of this approach was established in separate experiments comparing lattice vibration intensity and wafer mass.

Nitrous oxide decomposition experiments were performed in a fixed-bed microreactor that has been described previously (16). Product analysis was performed by using a chemiluminescent NOx analyser (Signal Instruments Model 4000) and a gas chromatograph fitted with a thermal conductivity detector (Pye Unicam PU4550). Catalysts were activated in flowing helium at 773 K for 1 h. The reactant mixture used to study the decomposition reaction comprised 1000 ppm of nitrous oxide in helium. Powdered catalysts were sieved to a mesh size of 0.6–1 mm, and the bed volume was 1 ml.

3. RESULTS

All samples show four characteristic X-ray diffraction features, at $2\theta = 2.0^\circ$, 3.7°, 4.2°, and 5.9°, consistent with a pore diameter of ca. 30 Å (11). However, where iron has been introduced during the synthesis step, the intensities of the two peaks at the highest diffraction angles are reduced, reflecting a decrease in the ordering of the hexagonal pore structure. This is consistent with changes in the electron micrographs shown in Fig. 1, where the areas of well-ordered hexagonal pores are smaller than in the parent MCM-41 material. It is also important to note, as Fig. 1 demonstrates for Fe-MCM-41-SYN, that none of the materials show evidence of particulate iron oxides. The BET surface areas and the BJH pore sizes obtained from nitrogen adsorption are listed in Table 1, which also gives information on the iron content of the materials studied. Introduction of iron, either during or after synthesis, decreases the surface area by up to 20%. The loss of surface area is believed to result from the introduction of iron into the pores, which will affect both the total pore volume and the surface area (17).

TABLE 1

Iron Content, Surface Area, and Mean Pore Size for the Materials Studied

Sample	Fe/wt%	Surface area/m^2g^{-1}	BJH pore size/Å
Si-MCM-41	—	1050	28
Fe-MCM-41-SYN	4	900	26
Fe-MCM-41-PS	3.5	850	27
Fe-ZSM-5	0.45	—[a]	—

[a] Nitrogen physisorption does not provide meaningful surface areas for microporous materials.

The infrared spectra of all of the mesoporous MCM-41 materials studied are characterised by a broad feature at 3600 cm^{-1}, which is due to clustered silanol groups or nests, and a much sharper band at 3742 cm^{-1}, which originates from stretching vibrations of terminal Si–OH groups (18). In Al-MCM-41 the intensity of the band at 3600 cm^{-1} is significantly decreased compared to that of purely siliceous samples, whereas the band at 3742 cm^{-1} is increased. For iron-containing materials, spectra are largely independent of whether activation takes place in a vacuum, in air, or in hydrogen, and representative results for the two Fe-MCM-41 samples and Fe-ZSM-5 are shown in Fig 2. The intensity of the broad feature at ca. 3600 cm^{-1} is reduced when iron is introduced after synthesis compared to the parent Al-MCM-41 material, which is consistent with earlier observations (14). Introduction of iron during synthesis results in a decreased intensity for this band. This is surprising, because introduction of iron is expected to increase the concentration of defect sites, which should result in a higher concentration of hydrogen-bonding silanol groups. By contrast, the band at 3742 cm^{-1} is reduced for the material modified with iron acetylacetonate, compared to the parent MCM-41. In purely siliceous samples modified with $Fe(NO_3)_3$ in methanol solution, this band increases in intensity (14).

Fe-ZSM-5 has a sharp band at ca. 3610 cm^{-1}, due to bridged Brønsted acid sites, which is absent in all of the MCM-41 materials. Also, the intensity in the 3700 cm^{-1} region is much lower in Fe-ZSM-5 than in any of the MCM-41 materials.

The results on the interaction with nitrous oxide are now presented. Figure 3 shows the FTIR spectrum of nitrous oxide at 1 mbar pressure, measured in the absence of any solid sample. There are several components in the range 2190–2260 cm^{-1} which fuse into the expected doublet as the pressure is increased to 10 mbar (19). In all of the remaining spectra, the contribution of gas-phase N_2O has been removed by subtraction. No nitrous oxide adsorption was detected on MCM-41 or Al-MCM-41, so any bands attributable to N_2O adsorption result from interaction with iron-containing sites.

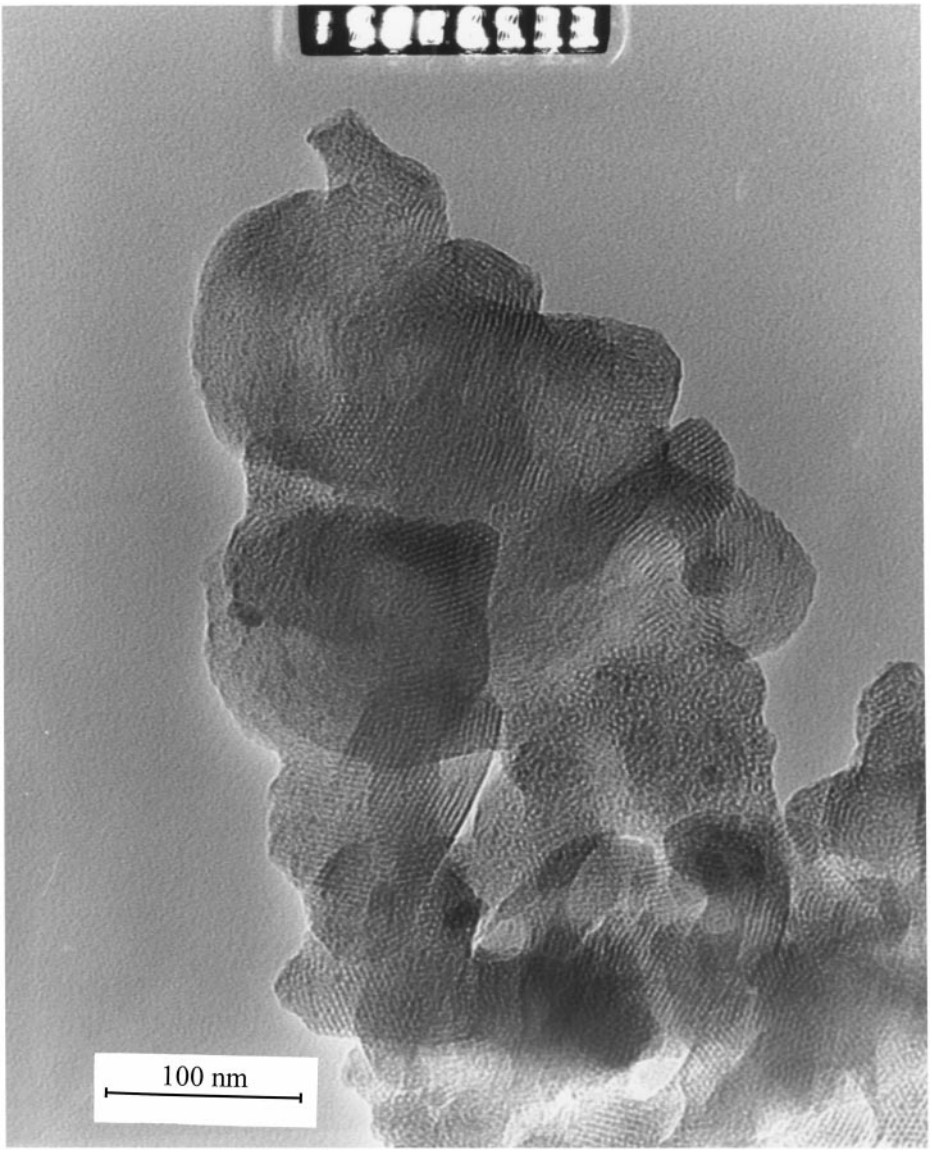

FIG. 1. Transmission electron micrograph of Fe-MCM-41-SYN, in which 4% weight of iron is introduced during framework synthesis.

Figure 4 shows spectra obtained during nitrous oxide adsorption on a range of materials at 303 K, after activation in a vacuum at 773 K. At the higher pressures studied, weak bands attributable to nitrous oxide adsorption are observed in the range 2230–2300 cm^{-1}. More surprising and interesting is the presence of much stronger bands observed at ca. 1830 cm^{-1} on Fe-MCM-41, and ca. 1876 cm^{-1} on Fe-ZSM-5. These positions are identical to those observed previously when *nitric oxide* (NO) interacts respectively with Fe-MCM-41 and Fe-ZSM-5 (13, 14). A further broad but weak feature is observed in the range 1620–1630 cm^{-1}, which has previously been identified as being due to adsorbed nitrogen dioxide or nitrate ions (20–22) formed by disproportionation reactions.

The observation of NO adsorption on these materials after exposure to nitrous oxide (N_2O) is entirely unexpected. An experiment has therefore been carried out in order to eliminate the possibility that NO adsorption results from its presence as an impurity in the N_2O supply, even though the manufacturer's specification is less than 1 ppm of NO impurity. Figure 5 compares the results of exposing Fe-MCM-41-SYN to 10^{-6} mbar of NO and to 10^{-5} mbar N_2O (equivalent to 10^{-11} mbar NO impurity), and similar intensities are observed at ca. 1825 cm^{-1}. Since the N_2O interacts at such a low pressure to yield spectra characteristic of adsorbed NO, any possible role for NO as an impurity in our N_2O supply can be ruled out. The spectra clearly arise from the room temperature

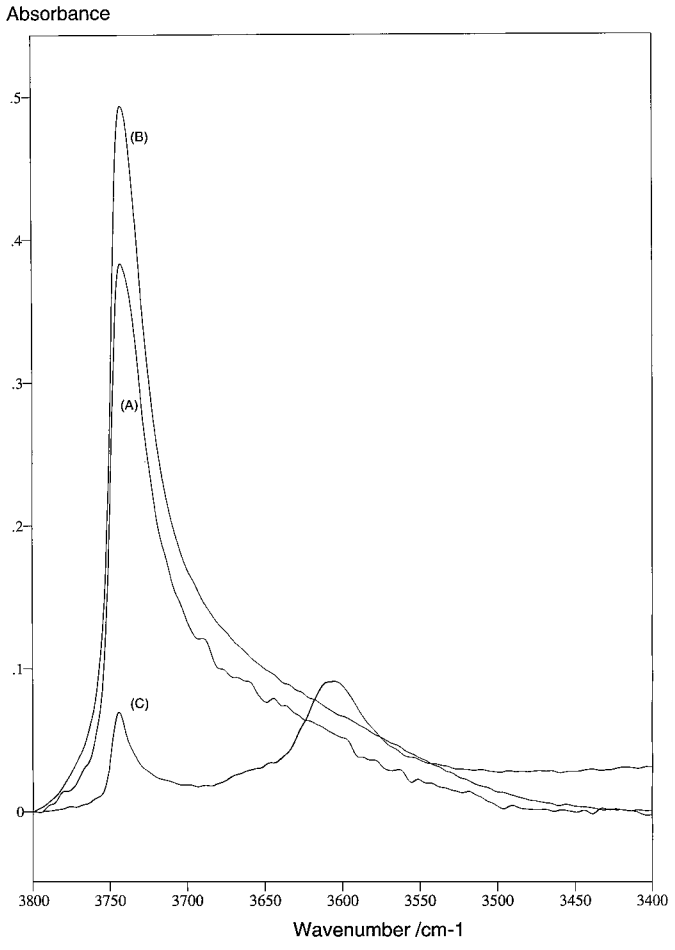

FIG. 2. FTIR spectra of samples activated *in vacuo* at 773 K: (A) Fe-MCM-41-PS; (B) Fe-MCM-41-SYN; and (C) Fe-ZSM-5.

conversion of N_2O to NO in the presence of iron-containing materials.

Once formed, nitric oxide may be desorbed by heating. In a fixed-bed microreactor, Fe-MCM-41-SYN was exposed to 1% N_2O in helium at room temperature for 75 min. The nitrous oxide flow was then switched off, and the sample temperature was increased in flowing helium. A small burst of NO was detected by the NOx analyser between about 420 and 470 K. This is the same temperature range where we have previously reported NO desorption from these materials (13, 14). Other experiments in the microreactor show that the N_2O decomposition reaction does not become catalytic until a temperature of ca. 770 K. The products of the catalytic decomposition are nitrogen and oxygen, and no nitric oxide is observed.

We have previously shown that Fe(II) present in both ZSM-5 and MCM-41 can easily be converted into Fe(III) by exposure to oxygen. On the other hand, activation of oxidised samples in a vacuum leads to reduction of Fe(III) species to Fe(II) (13, 14). However, no adsorbed nitric oxide is detected when oxidised samples of Fe-MCM-41 materials are exposed to N_2O, and this is not surprising, given that Fe(III) species have previously been demonstrated not to adsorb NO to any significant extent (13, 14).

4. DISCUSSION

In what follows, we consider first the properties of the hydroxyl groups and the location and structure of the iron species associated with the MCM-41 materials, and then discuss the unusual conversion of nitrous oxide to adsorbed nitric oxide that we have observed.

In agreement with earlier observations (14), the intensity of the hydroxyl stretching vibrations is significantly greater in the mesoporous MCM-41 material than in the microporous ZSM-5. However, even on MCM-41 materials containing aluminum, no bands assignable to bridging acidic hydroxyl groups were observed. Interestingly, the broad band at 3600 cm^{-1} which is attributed to clustered SiOH-like groups in hydroxyl nests is weakened in our Fe-MCM-41 materials compared to the case in the parent MCM-41, irrespective of whether iron is introduced during or after

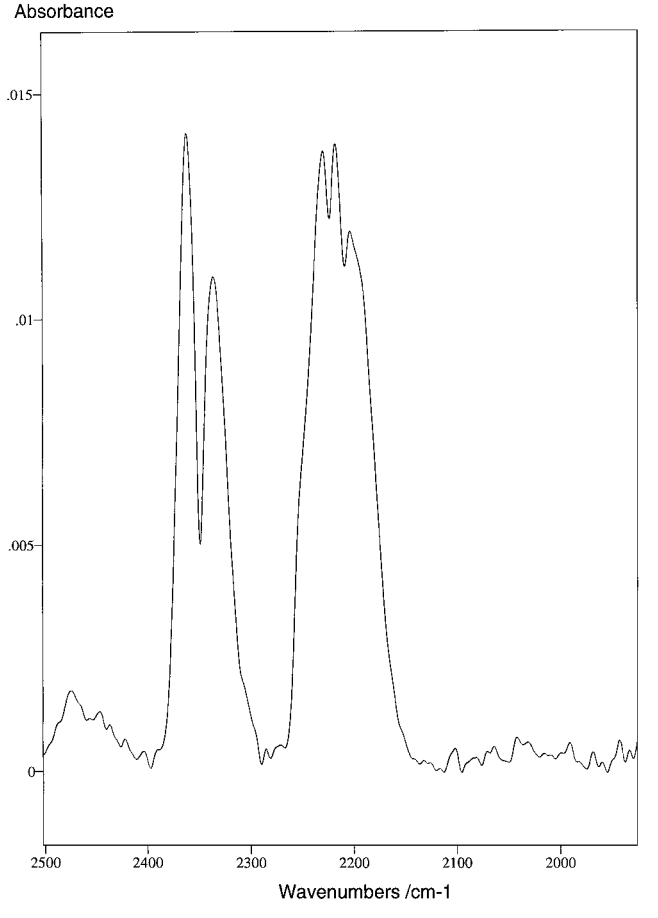

FIG. 3. Gas-phase spectrum of nitrous oxide, measured at 1 mbar pressure.

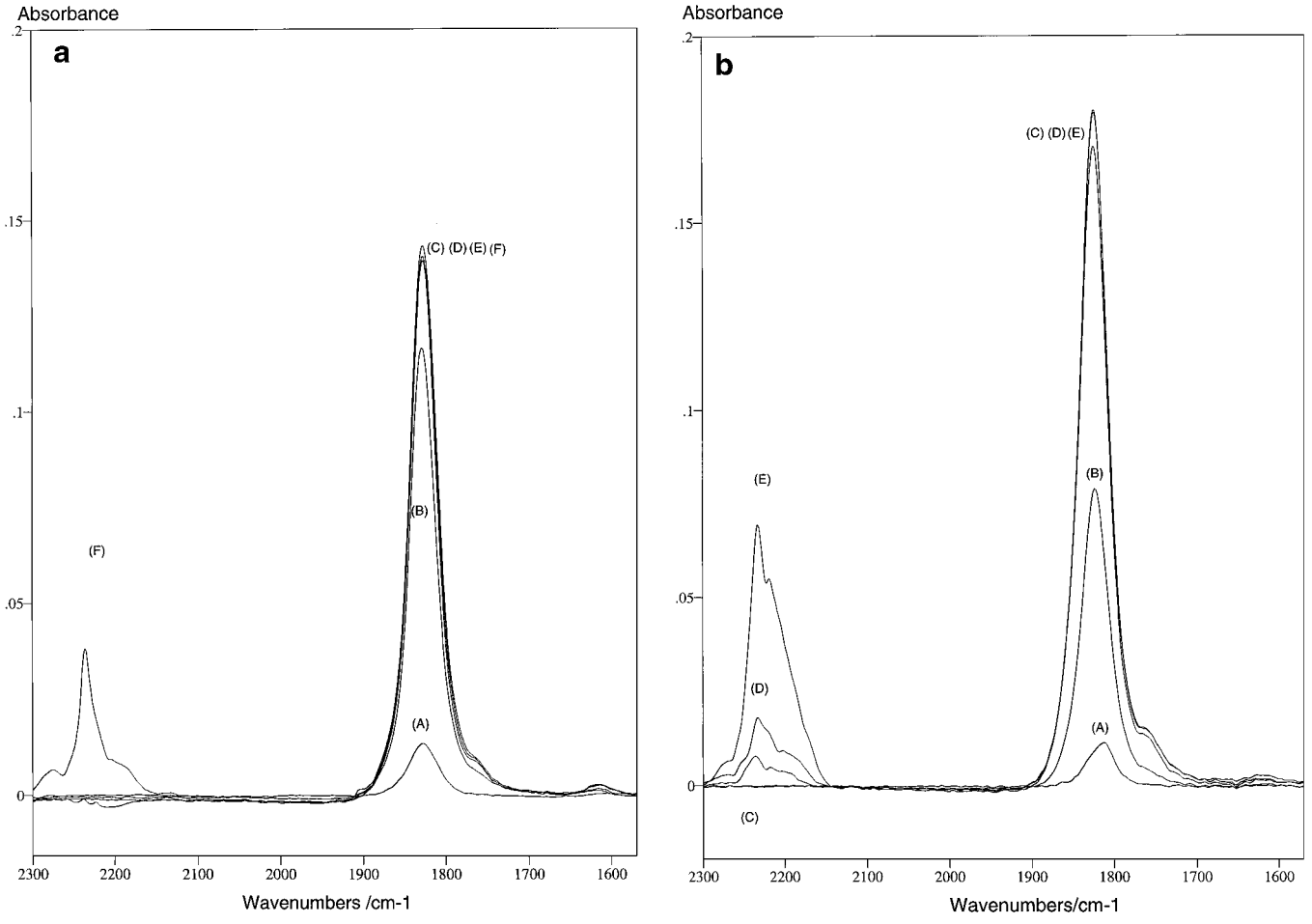

FIG. 4. (a) Normalised, difference FTIR spectra observed for Fe-MCM-41-SYN on exposure to N_2O at room temperature and different pressures: (A) 10^{-5} mbar; (B) 10^{-4} mbar; (C) 10^{-3} mbar; (D) 10^{-2} mbar; (E) 10^{-1} mbar; (F) 1 mbar. (b) As for (a), but for Fe-MCM-41-PS: (A) 10^{-5} mbar; (B) 10^{-4} mbar; (C) 10^{-3} mbar; (D) 10^{-1} mbar; (E) 1 mbar. (c) As for (a), but for Fe-ZSM-5. The noisier appearance of these spectra is due to the substantially lower iron content of this sample compared to the iron-MCM-41 materials—see Table 1.

synthesis of the framework. This is an indication that iron species are preferentially bound to these silanol nests, as we have reported for iron introduced after synthesis into purely siliceous MCM-41. Thus, the incorporation of iron during the MCM-41 synthesis appears to occur at strained positions in the walls, where several hydroxyl groups may occur in very close proximity.

Significant differences in the hydroxyl spectra are observed, dependent on whether iron is introduced from the acetylacetonate dissolved in toluene or from a methanolic solution of iron nitrate. In methanolic solutions, the intensity of the band at 3732 cm^{-1} was increased by treatment with methanol, whereas it was decreased by treatment with iron acetylacetonate in toluene. This is consistent with our findings (to be reported in detail elsewhere) that methanol reacts with the MCM-41 framework to form bound methoxy species and more isolated hydroxyl groups (14). The toluene solvent does not react with the MCM-41 framework, and the slight intensity decrease in the intensity of the band at 3740 cm^{-1} suggests a partial interaction of iron species with more isolated–OH groups.

Previous detailed studies of ZSM-5 (13) and purely siliceous MCM-41 (14) show that the iron cations may adopt a number of different structural environments. In ZSM-5, iron-oxo nanoclusters of typical size Fe_4O_4 are the majority species, and the NO absorption band occurs at 1880 cm^{-1}. A small number of isolated cations also occur, for which the NO absorption band is at 1840 cm^{-1}. In Si/MCM-41(MeOH), iron is present mainly in the form of isolated cations, on which the NO absorption band occurs at 1823 cm^{-1}. Only a very small number of nanoclusters exist in this material (14). Since in both cases, Fe-ZSM-5 (large concentration of clusters) and Fe-MCM-41 (mostly isolated), significant conversion of N_2O to NO occurs, we believe that both species, isolated cations, and clusters are acting as sites for the reaction. UV–visible spectroscopy and

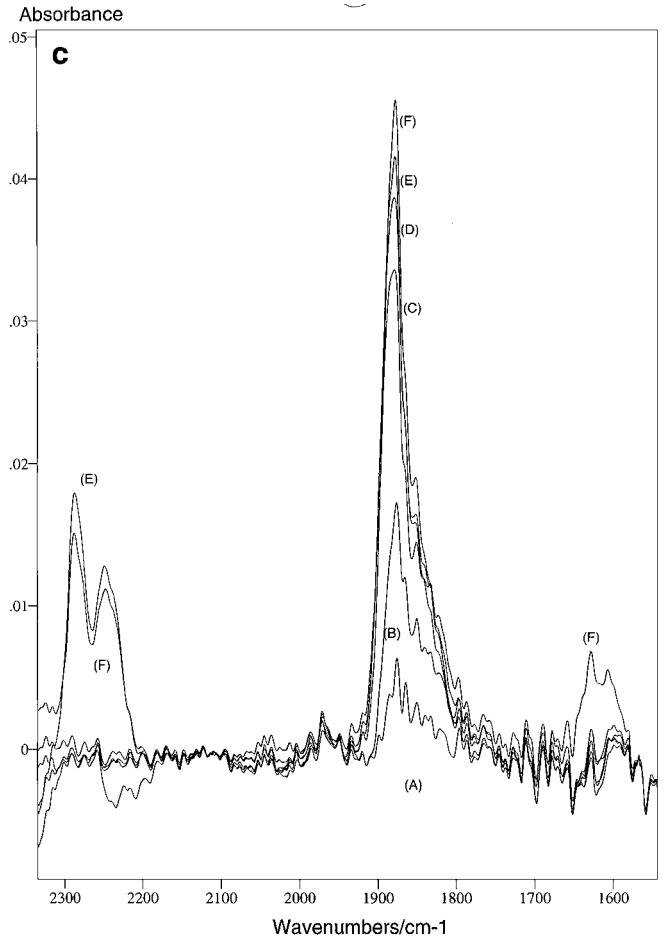

FIG. 4—*Continued.*

EXAFS measurements to be reported elsewhere suggest that in all of the MCM-41 materials studied here iron is present mainly in the form of isolated cations. The extent of iron aggregation, however, is likely to increase with the transition metal loading.

Molecular nitrous oxide is held only weakly both by the Fe-MCM-41 materials and by Fe-ZSM-5, and significant absorption bands are observed in the infrared spectra only at pressures of ca. 10^{-1} mbar or higher. Frequencies observed are typically higher than those of gas-phase N_2O, but the nature of bonding to the iron species is not clear. The results presented, however, show that nitrous oxide interacts at room temperature, both with Fe-MCM-41 and Fe-ZSM-5, to form adsorbed nitric oxide. Conclusive evidence for the formation of adsorbed NO is that the main N=O stretching frequency is known to occur at quite different positions in the infrared spectrum when it is adsorbed on Fe-MCM-41 (1823 cm^{-1} (18)), or nanoclusters in Fe-ZSM-5 (1880 cm^{-1} (13)). These are also the band positions that we observe when N_2O is allowed to react with these materials, as shown in Fig. 4. The reaction to form adsorbed NO occurs even at the lowest N_2O pressure studied, 10^{-5} mbar. It is only stoichiometric but it is highly efficient, and we have presented experiments that allow us to rule out impurity effects or other experimental artefacts.

In the MCM materials, differences in the absorption capacities for both NO and N_2O are observed, dependent on whether iron is introduced during (SYN) or after (PS) the framework synthesis step. For Fe-MCM-41-SYN, bands due to N_2O are found only at higher pressures, compared to those for Fe-MCM-41-PS. At lower pressures, the intensity of the NO band is higher in Fe-MCM-41-SYN, but lower at higher pressures. We believe that N_2O is first adsorbed at an iron cation and then converted to NO, which remains adsorbed on the same site. Conversion of N_2O to NO seems to be faster than that for Fe-MCM-41-PS, because at lower pressure the intensity of NO bands is higher and the intensity of the N_2O bands is lower for Fe-MCM-41-SYN than for the postsynthesis sample. Thus, more N_2O has been converted to NO. We do not understand the reasons for these small differences in the reactivity of the two samples. They

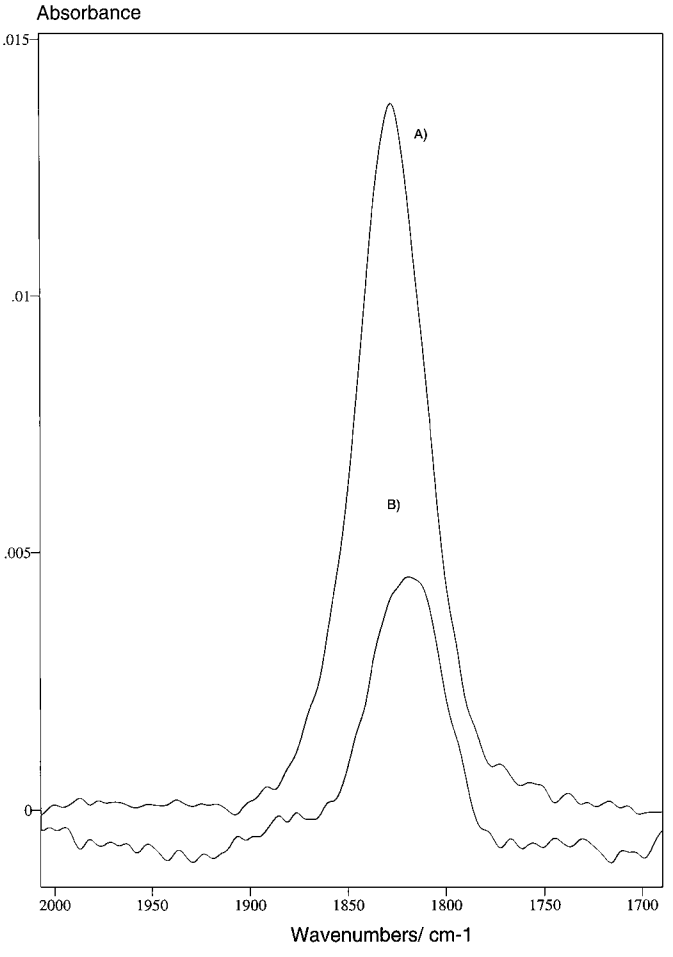

FIG. 5. FTIR difference spectra of the NO adsorption region for Fe-MCM-41-SYN after adsorbing: (A) N_2O at 10^{-5} mbar pressure; (B) NO at 5×10^{-6} mbar pressure.

may reflect subtle changes in the iron coordination environment indicated by small changes in EXAFS parameters and IR stretching frequencies.

At the highest pressures studied, we believe that the majority of accessible iron cations are covered with NO or N_2O. Although the iron content in Fe-MCM-41-PS is lower than that when iron is introduced during framework synthesis, a larger concentration of NO is observed, as the iron sites are thought to be more accessible.

Reaction between adsorbed nitrous oxide and the iron-containing materials to form adsorbed nitric oxide has not been reported before. As noted above, the reaction takes place when the materials are in their reduced form, and iron is present as Fe(II). We therefore propose that the reaction is

$$N_2O \rightarrow NO_{(ads)} + 0.5N_2.$$

The fate of the nitrogen atoms is not known. They may remain as an adsorbed species; however, they most probably combine and desorb as N_2. This reaction sequence is thermodynamically favourable, since the free energy change for

$$2N_2O \rightarrow 2NO + N_2 \quad \text{(all species in the gas phase)}$$

is $\Delta G_o^{298} = -35.7\ \text{kJ mol}^{-1}$. The adsorption of NO on Fe(II) species is exoenergetic, further increasing the thermodynamic driving force.

We have not been able to make the N_2O decomposition reaction catalytic at low temperatures. Nitric oxide does not desorb at room temperature and therefore self-poisons the potential catalyst against further activity. At higher temperatures, once NO does desorb from the catalyst, we believe that the interaction of nitrous oxide with the iron cations, already weak at room temperature, has become too weak for it to adsorb and react.

As with many oxide materials containing transition metal cations, Fe-MCM-41 and Fe-ZSM-5 show activity for the catalytic decomposition of nitrous oxide into its elements, but only at temperatures in excess of ca. 700 K (1, 3, 4). The course of that interaction is thus quite different from that reported here, and the mechanism is also likely to be different, almost certainly involving the fission of the N–O bond, rather than the split into N and NO fragments that we observe here. Our results suggest that a cyclic temperature swing process for the conversion of N_2O to NO can be envisaged, whereby adsorbed NO is formed by interaction of N_2O with Fe-MCM-41 at room temperature, and the product desorbed by heating to a temperature of ca. 420–470 K. This could be practically advantageous, as the selective reduction of NO to nitrogen can be carried out at lower temperatures than are normally needed for N_2O decomposition.

TABLE 2

Relative Intensities of the Infrared Adsorption Bands for Adsorbed NO Observed on the Different Materials Studied, Normalised for Different Iron Contents and Wafer Thicknesses

	Sample		
	Fe-MCM-41-SYN	Fe-MCM-41-PS	Fe-ZSM-5
Relative intensity	0.024	0.045	0.050

A measure of the extent to which the N_2O to NO conversion occurs can be gained by examining the intensity of the absorption bands due to NO. Table 2 compares the three samples studied, providing relative intensities that are normalised both for wafer thickness and iron content. The results are similar for Fe-ZSM-5 and for Fe-MCM-41 where the iron has been introduced after framework synthesis. A much lower figure is noted, however, for Fe-MCM-41-SYN, suggesting that some of the iron in this sample has been buried in the structure during synthesis. This correlates with the less well ordered nature of this sample. The similar results for Fe-MCM-41-PS and Fe-ZSM-5 suggest that the reaction may occur at both isolated Fe(II) ions and iron-oxo nanoclusters.

ACKNOWLEDGMENTS

We are very grateful to Philippe Trens (Reading University) for help with the MCM-41 synthesis and to Ian Burton (previously at Nottingham Trent University, now at the Queen's University of Belfast) for carrying out the nitrous oxide decomposition experiments. We also acknowledge the financial support of the Engineering and Physical Sciences Research Council.

REFERENCES

1. Kapteijn, F., Rodriguez-Mirasol, J., and Moulijn, J. A., *Appl. Catal. B: Environ.* **9**, 25 (1996).
2. Xie, S., and Lunsford, J. H., *Appl. Catal. A: General* **188**, 137 (1996).
3. Akbar, S., and Joyner, R. W., *J. Chem. Soc., Faraday Trans. 1* **77**, 803 (1981).
4. Rauscher, M., Kesore, K., Mönning, R., Schweiger, W., Tissler, A., and Turek, T., *Appl. Catal. A: General* **184**, 249 (1999).
5. Mauvezin, M., Delahay, G., Coq, B., and Kieger, S., *Appl. Catal. B: Environ.* **23**, L79 (1999).
6. Valyon, J., Millman, W. S., and Hall, W. K., *Catal. Lett.* **24**, 215 (1994).
7. See, e.g.: Tanaka, T., Okuhara, T., and Misono, M., *Appl. Catal. B: Environ.* **4**, L1 (1994).
8. Sugiyama, S., Abe, K., Hayashi, H., Matsumura, Y., and Moffat, J. B., *J. Mol. Catal. A: Chem.* **144**, 347 (1999).
9. Panov, G., Kharitonov, A. S., and Sobolev, V. I., *Appl. Catal. A: General* **98**, 1 (1993).
10. Pophal, C., Yogo, T., Yamada, K., and Segawa, K., *Appl. Catal. B: Environ.* **16**, 177 (1998).
11. Grün, M., Unger, K. K., Matsumoto, A., and Tsutsumi, K., *Microporous Mesoporous Mater.* **27**, 207 (1999).

12. Kenvin, J. C., and White, M. G., *Langmuir* **7**, 1198 (1991).
13. Stockenhuber, M., and Joyner, R. W., *J. Phys. Chem. B* **103**, 5963 (1999).
14. Stockenhuber, M., Hudson, M. J., and Joyner, R. W., *J. Phys. Chem. B* **104**, 3370 (2000).
15. Jentys, A., Kleesdorfer, K., and Vinek, H., *Microporous Mesoporous Mater.* **27**, 321 (1999).
16. Connerton, J., Stockenhuber, M., and Joyner, R. W., *J. Chem. Soc., Chem. Commun.* 185 (1997).
17. Mokaya, R., and Jones, W., *J. Mater. Chem.* **9**, 555 (1999).
18. Jentys, A., Pham, N. H., and Vinek, H., *J. Chem. Soc., Faraday Trans.* **92**, 3287 (1996).
19. See the Galactic Industries database of infrared spectra at www.galactic.com.
20. Hoost, T. E., Laframboise, K. A., and Otto, K., *Appl. Catal. B: Environ.* **7**, 79 (1995).
21. Kucherov, A. V., Slinkin, A. A., Kondreatev, A. A., Rubinsthein, T. N., and Minachev, K. M., *Zeolites* **5**, 320 (1985).
22. Aylor, A. W., Larsen, S. C., Reimer, J. A., and Bell, A. T., *J. Catal.* **157**, 592 (1995).